Telocytes Promote the Metastasis of Hepatocellular Carcinoma by Activating ERK Signaling Pathway and Sponging miR-942-3p to Impact MMP9

Ying Xu
Shandong Cancer Hospital: Shandong Cancer Hospital and Institute https://orcid.org/0000-0002-8941-7560

Hu Tian (tianhu6585@163.com)
Shandong First Medical University

Chao Guang Luan
Ji'nan Municipal Three Hospital

Kai Sun
The First affiliated hospital of shandong first medical university

peng Jin Bao
Shandong First Medical University(shandong academy of medical sciences)

Hua Yu Zhang
Shandong University of Traditional Chinese Medicine Affiliated Hospital

Nan Zhang
Shandong University of Traditional Chinese Medicine Affiliated Hospital

Research

Keywords: Telocyte, platelet-derived growth factor, hepatocellular carcinoma, ERK signaling pathway, matrix metalloproteinase-9, miR-942-3p

Posted Date: April 8th, 2021

DOI: https://doi.org/10.21203/rs.3.rs-364558/v1

Abstract

Background: Hepatocellular carcinoma(HCC) in China is considered as a familiar malignant tumor with poor prognosis, high metastasis and disease relapse. Telocytes(TCs) have been verified to participate in progresses of tumorigenesis, invasions and migrations by secreting functional proteins and transmitting cell-to-cell information. Extracellular signal-regulared protein kinase(ERK) signal pathway is a vital mechanism driving cell proliferation, metastasis and apoptosis, but whether this molecular signaling mechanism contributes to matrix metalloproteinase-9(MMP) expression of TCs remains unclear.

Methods: Telocytes and MMP9 expression in the liver cancer tissues are measured by immunohistochemistry assay, Westen blot assay and RT-PCR technique, meanwhile primary telocytes from liver para-cancer tissues are cultured in vitro. To demonstrate the function of telocytes for hepatocellular carcinoma, the metastatic cancer animal model is established by three typs of liver cancer cell-lines in vivo.

Results: In our study, we elucidate that TCs in the para-cancer tissue can promote the metastasis of HCC cells by MMP-9 expression, in vitro and in vivo. PDGF derived from HCC cells has a capacity to activate Ras/ERK signaling pathway of TC as a result of accelerating MMP-9 expression, but it's no significant for proliferative potential and apoptotic rate of TCs. While tyrosine kinase inhibitors and miR-942-3p suppress MMP-9 expression to make loss functions of TCs. Various mutations of TCs are also tested and single nucleotide polymorphisms of MMP-9 may be the potentially molecular mechanism of increasing protein expression in the invasive process of HCC.

Conclusion: Our results demonstrate two potential mechanisms between HCC cells and TCs, suggesting that TC is a novel marker and target on deciphering reasons of cancer metastasis.

Background

Globally, liver cancers are the sixth most familiar cancers and rank fourth in terms of cancer related mortality[1], and the World Health Organization estimates that more than one million patients will die of it in 2030[2]. Metastasis is an common lethal factor for most malignant carcinoma. The secondary germination in distant organs requires multiply steps process such as intruding into the blood circulation system after tumor angiogenesis, sustainable growth with inexhaustible viability, and high-intensively colonized power[3]. Cancer cells could overcome multitudinous obstacles by a way of alternating surrounding environment and regulating peripheral cells to establish appropriate conditions for metastasis. Although various efforts have been conferred to demonstrate the molecular mechanism of HCC, we are still accustomed to diagnose it at the clinical stage, distant metastatic phase and post-surgical recrudesces[4]. Imminently, a novel biomarkers related to metastasis and prognosis of HCC, and new target regulations of promoting invasion and migration to normal tissues are necessary.

Telocytes(TCs), deriving from interstitial Cajal-like stem cells(ICLC), are a novel type of mesenchymal cell with several long□thin and beaded-like telopodes and extensively exist in the most of mammal animals'

organ[5-9]. According to previous researches, TCs are confirmed positive for CD34, CD117, platelet-derived growth factor receptor(PDGFR) and negative for CD28, Vimentin and NOS in the hepatic tissue, kidney and vascular tissues[10]. These bio-marks are utilized for TCs' identification[11-13]. Potential functions of TCs have been discovered to construct the basis support of arteries[14], participate in the pathological process of chronic wound healing[12,15], involve in transmit signaling information by autocrine and paracrine approaches[16,17], and result of cell steatosis in atherosclerotic disease[10]. The study of TCs in the tumorigenesis and development, the current exploration is only limited on the morphological and quantitative alterations of TC in tumors[18,19] and restricted to activate or inhibit signaling pathways of TC[20]. For instance, hyperplastic TCs were found as the physiological counterpart on the neoplasia of inflammatory fibroid polyps and PDGFRA mutant gastrointestinal stromal tumor[19]. Furthermore, TCs with steroid hormone receptors on membrane involved in uterine leiomyoma growth by changing their density and local homeostasis[18]. Nonetheless, present studies only concentrate on the morphology, magnitudes, superficial bio-markers and ultrastructure changes of TCs in distinct organs, but the mechanisms of why TCs have capabilities to promote tumor growth and metastasis and which molecular variants happen inner TCs, were still unknown and imminently investigated.

Extracellular matrix(ECM) procides mechanical and biochemical support to cells and constructs homeostasis of peripheral tissues, and they contain matrix metalloproteinases(MMPs), heparanases and aggrecanases, among others[21,22]. MMP-9, one of MMPs, not only participates in matrix remodeling of tissues[23,24] but also involves in migration, in vasion and tumorigenesis of cancer[25,26]. MMP-9 can be secreted by ICLC such as TCs through the way of homocellular junctions to interact with other surrounding cells. Downregulating the density of MMP-9 suppressed the metastasis of HCC[27,28]. Focusing on the mechanism of MMP-9 expression, more than one signaling pathways contribute to promote or inhibit it, including PI3K/AKT/NF-κB signaling pathway, transforming growth factor-beta(TGF-β)/SMAD signaling pathway[29,28,30]. What's more, inhibition of ERK led to reduce MMP-9 expression and gain-of -function reversed by eliminating MAPK related inhibitors in the fibrosarcoma disease[31]. In head and neck squamous cell carcinoma, iron exhibited to medicate MMP-9 by ERK1/2 signaling pathway[32].

The correlation and interaction of TCs and HCC remain undetermined. Therefore, the aim of our study is to explore a new target to disclose the mechanism of metastasis of HCC and discover the signal transduction between HCC and TCs. With preliminary experiments, we audaciously hypothesis that HCC cells secreted PDGF, binding with PDGFR on TCs and resulted in accelerating MMP9 expression, the latter played a pivotal role in tumor migration and invasion to distance. Additionally, molecular mechanism of MMP9 expression of TCs was an extremely complicated progress including microRNA(miRNA) regulation and a characteristic signaling pathway, so we also highly conjecture that downstream target gene of MMP9-related miRNA simultaneously participated in adjusting the expression of MMP9. Therefore, in order to verify these speculations, we tested TCs density and MMP9 expression by immunohistochemistry, immunofluorescence and Westen blot assays, and analyzed their relationship with the overall survival(OS) phase. Furthermore, we construct experiments in vivo and in vitro to explore the influence and mechanism of TCs with MMP9 in metastasis of HCC.

Materials And Methods

Clinical samples

Between January 2018 and June 2020, Surgical tissues were collected at the first affiliated hospital of Shandong first Medical University from 132 patients with hepatocellular carcinoma disease confirmed by fast pathology biopsy during the operation after patients' signed informed consents were obtained. All fresh tissues were restored immediately on the refrigerator of -80℃ and anonymized before transfer to the laboratory for further processing. All the demographic data, including age, sex, clinical classification, survival time, and relative follow-up visits were gathered. All control subjects were followed up for two and a half years and were free of liver malignancy.

Primary TCs Culture

Fresh samples from liver para-cancer tissues and hepatic hemangioma tissues(as the control group) after patients' operation were selected and cut into fragments, and incubated with 5 mg/ml collagenase type II (Sigma-Aldrich, St. Louis, MO, USA) for 10min. PBS without calcium and magnesium(pH 7.4， G0002，Servicebio, USA) washing twice and centrifuged at 1000 r.p.m., 5min, then re suspended in DMEM with 10% foetal calf serum. The BJ-40 capillary glass tube (1.0 mm outer diameter, 0.8 mm inner diameter) was soaked in 1 mol/L hydrochloric acid for 24 h, then rinsed continuously with ultrapure water, dried at 65°C and autoclaved. Under 200x magnification of the microscope and selected cells to 0.2 mL centrifuge tube containing 2μL of lysate according to the morphology of TCs[33,34].

Liver TCs isolation and identification

After mature C57BL/6 mice(No.4432, Weitonglihua animal company, Beijing, China) were killed with anaesthetic. The hepatic tissue were isolated under sterile conditions and collected into sterile tubes containing DMEM (Gibco-8120217, NY, USA), Suppl.ed with 100 UI/ml penicillin, 0.1 mg/ml streptomycin (20201013, Kaisu biology Co Ltd., Jiangsu, China), transported to the cell culture laboratory. Dispersed cells were separated by filtration through a 40-m-diameter cell strainer(CLS431751，Falcon, NJ, Germany), collected by centrifugation at 1000 r.p.m., 5min., and resuspended in DMEM, Suppl.ed with 10% foetal calf serum, 100UI/ml penicillin, 0.1 mg/ml streptomycin (Sigma-Aldrich). Cells were distributed in 25cm^2 plastic culture flasks, at a density of 1×10^5 cells/cm^2, and maintained at 37°C/5% CO_2 atmosphere until becoming semi-confluent. Culture medium was changed every 48hrs. The typical TC were photographed by auto-microscopy per 12hrs. After cell adhesion on the plate, Cells were selected, purified and further amplified to the next experiment. The TCs were identified according to the morphology and immunofluorescent staining assays. The protocol followed by the hereinafter.

Lentivirus production and infection

To build recombinant lentivirus, 293T cells were cotransfected with progresses of package, envelop, and expression. The virus-containing supernatant was harvested and concentrated by ultracentrifugation. The

viral stock was Suppl.ed with 8 mg/mL of polybrene for infections .

Cell Transfection

In order to gain stable experimental cell lines, the primary TCs from hepatic tissues(from mice) transfected with SV40 large and small T antigen to constructed TC^{SV40}. The culture medium of TC^{SV40} cells was Dulbecco's modified Eagle's medium/F12 with 10% fetal calf serum (Gibco-8120330, NY, USA) Suppl.ed. HepG2, SNU182 and SK-HEP-1 cell-Lines were cultured in DMEM(GIBCO，Beijing, China) Suppl.ed with 10% FBS, 100 U/ml of penicillin, and 100 μg/ml of streptomycin and then Cells were placed in a humidified atmosphere containing 5% CO2 at 37°C. When cells reached 60– 80% confluence, positive and stable transfectants were selected for further study.

RNA extraction and qRT-PCR analysis

To verify the mRNA expression level of MMP2, MMP3, MMP9, MMP11 and MMP14 in HCC tissues and para-cancer tissues, qRT-PCR analysis was performed. Total RNA was extracted from tissues using Trizol reagent (CW0581, Kangweishiji company, China) according to the manufacturer's protocol. Reverse transcription and cDNA amplification were performed using the SYBR Master Mixture (CW0957, Kangweishiji company, China), respectively, according to the manufacturer's guidelines. The β-actin genes were used as endogenous controls. A HiFiScript Primer Assay (CW2569, Kangweishiji company, China) was used to assay MMPs and β-actin(Suppl. Table 1).

RNA interference

For miR-942-3p test, mature miRNA sequence was found by miRBase database, shRNAs and mimics of indicated miRNAs were obtained by RiboBio Company (Shanghai and Wuhan, China). Transfection with shRNAs and miRNAs was completed using riboFECT™ CP (RiboBio) according to the manufacturer's instructions.

Luciferase assay

For 3' -UTR analysis, cells were cotransfected with psiCHECK-2–based construct and pre-miR-942-3p or a negative control. Luciferase assay was conducted with the Dual-Luciferase Reporter Assay System (Promega). Luciferase miRNA Target expression vector (Promega, Madison, WI, USA) to construct the reporter vectors: MMP-9 wild type (WT) , MMP-9 mutant (MUT) and negative vectors-mimics(NC).

Western blot analysis

Human hepatocellular cancer tissues with para-cancer tissues were fetched out from the -80℃ condition, thawed and resuspended using lysis buffer (20% Glycerol, 4% SDS in 100 mM Tris Buffer, pH 6.8). Cell extracts were boiled for 10 min in loading buffer and then equal amounts of cell extracts were separated on 10% sodium dodecyl sulfate polyacrylamide gel electrophoresis gels. Separated protein bands were transferred onto polyvinylidene fluoride membranes. The primary antibodies against MMP2, MMP3,

MMP11, MMP9, MMP14 and GAPDH were diluted according to the instructions for each of the antibodies and incubated overnight at 4°C. Then, horseradish peroxidase-linked secondary antibodies were added and samples were incubated at room temperature for 2 h. The membranes were washed with phosphate-buffered saline (PBS), and the immune-reactive bands were colored using an ECL-PLUS/TM (Amersham company, UK) according to the manufacturer's instructions. The relative protein levels between cancer tissues and para-cancer tissues were normalized to GAPDH concentrations. Three separate experiments were performed for each clone. Furthermore, the primary antibodies against Bax and Cleaved-caspase-3 were incubated for cell apoptosis test(Suppl. Table 6).

Immunohistochemistry (IHC) staining

Formalin fixed paraffin-embedded primary tumor tissue with para-cancer tissue were utilized for IHC. For heat-induced antigen retrieval, slides were soaked in citric acid buffer and heated keeping 1300w for 2 min. After quenching endogenous peroxidase activity with 3% H_2O_2. Specimens were incubated with antibody at 4°C overnight. Specific signals were developed with second-antibody using diaminobenzidine as chromogen(Suppl. Table 6). Sections were then counterstained with hematoxylin and observed under light Microscope(XSP-C204, CIC, China). Slides were scanned using laster scanning confocal microscope (Eclipse Ti-E, Nikon, Japan) with 40×magnification. Datum were quantified in immunohistochemistry digital slides with Leica Aperio positive pixel count algorithm using whole slide analysis (PANNORAMIC DESK/MIDI/250/1000, 3DHISTECH, Hungary).

Immunofluorescence(IF) staining

All sections were incubated in 2 changes of xylene at 15 min each. A dehydrator was used to dehydrate the sections in 2 changes of pure ethanol and were immersed in EDTA antigen retrieval buffer (pH 8.0, G1206/G1203, Servicebio, USA). The slides were incubated with primary antibodies to double stain for CD34, CD117, PDGFR-α and MMP9 overnight at 4°C and then with secondary antibody after washing three times with PBS(Suppl. Table 6). Under microscopy, images were collected using fluorescence microscopy (NIKON ECLIPSE C1, Tokyo, Japan) with an imaging system (NIKON DS-U3, Tokyo, Japan). Images were captured at 1 to 400 magnification (Microscope Camera XSP-C204, Olympus Europa GmbH, Hamburg, Germany).

Transwell assay

For invasion assays, Transwell migration chambers and Matrigel coated chambers(Becton Dickinson, Waltham, MA) were used. Briefly, 5×10^4 HCC cells were seeded into the upper chamber in serum-free culture medium. The lower chamber was filled with 5×10^4 TCs completed medium with 10% FBS. After 48 h for the invasion assay, cells that have invaded through the membrane were stained with 1% crystal violet and counted in the microscopy(CKX-51,OLYMPUS company, Japan).

CCK-8 cell counting assay

TCs in logarithmic phase were digested and made into cell suspensions. After uniform spreading, the cells were incubated and then 10 μ L of 5 mg/mL cell counting kit-8(CCK-8)(HY K0301, MCE, Shanghai, China) was added to the wells starting from the second day after spreading and 4 h before the termination of the incubation. The OD value was measured at 450 nm by enzyme marker after 4 hours.

Wound healing assay

Use a marker pen on the back of the 6-well plate uniformly with horizontal lines. Add approximately 2.5 × 10^5 HCC cells to the wells and overnight to reach 100% fusion rate. Prepare co-culture cells-TC^{SV40}, wash the cells 2-3 times with PBS after digestion, resuspending with serum-free medium and add co-culture chambers. MMP9 inhibitor group was a concentration of 3uM, adding each group of co-culture chambers into the corresponding wells. Every chambers incubated in 37℃ 5% CO_2 incubator for 48hr. The area was counted using Image J software.

In vivo models

For building metastatic lung cancer, 1 × 10^7 HepG2 cells in 100 μl of PBS were injected into the tail veins of BALB/c-nu mice(No.4272, Weitonglihua animal company, Beijing, China). 6 × 10^4 TCs in 50 μl of 0.9% normal saline were injected into mouse tail vein per 7 days after HepG2 cells injection. The mice were sacrificed on day 42. Lung tissues were resected, photoed and fixed with 4% paraformaldehyde, and then strained with hematoxylin and eosin (HE). For subaxillary transplantation, HepG2 cells were injected into the right axilla of nude mice and 6 × 10^4 TCs in 50 μl of 0.9% normal saline were injected around local tumors per 3 days and TCs with MMP9 inhibitor group built as the compared group. After 28 days, these mice were sacrificed to gain axilla transplanted tumors which were measured weights and volumes(maximum axis × minimum $axis^2$ × 1/2).

Whole-exome Sequencing Technique

Experimental Flow

A cohort of 23 patients with HCC who underwent surgical resection between 2019 and 2020. Primary culture TCs were selected from fresh para-cancer tissues of Genomic DNA samples of acceptable quality were randomly interrupted by ultrasonic high performance sample processing system (Covaris) into fragments with a major peak of about 200bp-300bp. Subsequent DNA fragments were then end-repaired by adding an "A" base at the 3' end and a library splice at both ends. An appropriate amount of hybridization library was captured and enriched with the exome chip, and the unenriched fragments were eluted and amplified, and the whole exome was captured. The amplification products were subjected to Agilent 2100 bioanalyzer instrument (Agilent DNA 1000 Reagents) and QPCR quality control. We used the Illumina HiSeq family of platforms to perform high-throughput sequencing of each qualified library and to ensure that the data volume of each sample was up to standard. The raw image data obtained from sequencing was converted into raw reads (raw reads) by Illumina Base Calling software, i.e. double-end reads (paired-end reads). The data were stored in FASTQ file format, called raw data.

Variant Calling and Bioinformatics Analysis

The information analysis started with the sequenced downstream data. The raw data contained adapter sequences, bases of low sequencing quality, and undetected bases (expressed as N). Next, the clean data of each sample was compared to the reference genome using the alignment software BWA(Burrows-Wheeler Aligner)[35] to obtain the initial alignment result file in BAM format. To ensure the accuracy of variant detection, we followed the optimal variant detection analysis procedure recommended by the official website of GATK. Based on the alignment results, the evaluation indexes such as sequencing depth, coverage, and alignment rate of each sample were counted. In the process, we wield HaplotypeCaller of GATK v3.4.0, including SNPs(single nucleotide polymorphism) and InDels, and filtered the raw variant detection results with high confidence(Suppl. table 3,4). Next, the variant results were annotated and impact predicted using the in-house software AnnoDB, as well comparison of different types of sample sets using the genome visualization software IGV(Integrative Genomics Viewer; Suppl. figure 3-F).

Statistical analyses

SPSS20.0 was utilized for the statistical analyses. Quantitative value was recorded as the mean ± standard(SD). Two-tailed Student's t-tests, paired t-tests, chi-square tests, and multivariate analysis were used to assess the differences among groups. Pearson correlation analysis was used to analyze MMP9 expression with TCs number in HCC tissues. Survival curves were drawn by the Kaplan–Meier analysis and statistical significance was considered as $P < 0.05$.

Results

The identification of TCs

The live-origin TCs were identified with unique morphological features under the light microscope(Fig1 A,B) and cellular surface biomarkers CD34、PDGFR-α and CD117 by immunofluorescence assay(Fig1 D,E,F). TCs possessed an unique feature with several long and thin telopodes which were special characteristics against fiberocyte and epithelial cells(Fig1 C)[36].

The diversity and correlation analysis between Telocytes and MMP-9

in HCC tissues.

In order to verify the number changes of telocytes in HCC tissues, we chose 132 specimen by immunofluorescence assay to calculate the quantity of CD34-positive telocytes in the HCC tissues and para-cancer tissues(Fig2 A-a,e). Visibly, the number of telocytes in the HCC tissues were rare compared with them in the para-cancer tissues, and it had significant by paired *t* test statistic assay(*t* value =57.640, *p* <0.0001, Fig2 B). MMP-9 protein was also detected by immunohistochemistry and immunofluorescence assays both in the HCC and para-cancer tissues, the MMP-9 protein expression index of former tissues was lower than it of latter tissues(*t* value =138.600, *p* <0.0001, Fig2 A,B). Furthermore, MMPs family

including MMP2, MMP3, MMP9, MMP11and MMP14 were also utilized to represent the differences between HCC tissue and para-cancer tissue by Wesen blot assay, qRT-PCR analysis and immunohistochemistry staining. Interestingly, not all proteins of MMPs family had similar expressions in HCC and para-cancer tissues(Fig2 C,D,E) : there was scarce discrepancy of MMP2 and MMP14 expression; MMP3 protein expressed lowly in the para-cancer tissue but highly in the HCC tissue; MMP11 protein expression was more in the HCC tissue, but the result was adverse by qRT-PCR analysis. Additionally, the correlation of MMP9 protein and telocytes was demonstrated through Pearson's correlation statistic analysis both HCC tissues and para-cancer tissues(Table 3), and this positive correlation between MMP9 protein and telocytes was a critical and high-level TC precondition for following studies. In order to clarify potential clinical correlations among MMP9 protein, telocytes and HCC metastasis patients, we analyzed quantities of telocytes from 93 cases with HCC metastasizing patients and 39 cases without metastasizing patients. The count of telocytes and MMP9 protein expression in the para-cancer tissue were obviously higher in metastasizing samples than them in non-metastasizing samples(Fig 3 B), and MMP9 protein expression allocated surrounding telocytes on scans of immunofluorescence staining(Fig 3 A). Whether high number of telocytes were relative with cancer metastasis in the HCC para-cancer tissues , we factitiously made two hierarchical classifications of telocytes: low-count $\leq 8/\mu m^2$ high-count $> 8/\mu m^2$(Table 1) . We found that age of high-telocyte group was younger than it of low-telocyte group(65.510±0.934 VS 75.763±1.640 years, p=0.001), and the former group was more easily inclined to distant metastasis compared with the latter group. High-telocyte group accompanied by higher MMP9 protein expression contrast with low-telocyte group(7.859±0.349 VS 7.138±0.273, p=0.001; Table 1). The OS in the high-telocyte group was statistically significant shorter than that in the low-telocyte group, coincidently the OS outcome of MMP9 protein level represented analogously like telocyte groups(10.455±3.290 VS 19.932±2.028 months; Fig 3 C). Multivariate analysis, including age, sex, metastasis stage, MMP9 protein expression and TCs number, demonstrated that MMP9 and TCs were independent hazard factors in HCC patients(Table 2).

Telocytes promoted HCC migration and invasion by MMP9 expression

To investigate the effects of TCs on HCC migration and invasion, we performed Wound healing migration(Fig 4-A) and Transwell invasion assays(Fig 4-B), which indicated that TCs promoted cell migratory and invasive abilities of HepG2, SNU182 and SK-HEP-1 cells, meanwhile inhibiting MMP9 expression attenuated these impacts. To functionally validate roles of TCs to HCC cells, we performed in vivo assays using xenograft mouse models by injecting HepG2 cells and TCs to mice axilla(Fir 4-C). After 21days, the weight and volume of HepG2 tumor with fifth TCs injections were obviously biggest than only HepG2 tumor and tumor with MMP9 inhibitor(p<0.01;Fig 4-D,E). There were no significant of migration and tumor growth between HepG2 tumor group and tumor with MMP9 inhibitor group(p>0.05), so TCs impacted HCC activity depending on MMP9 expression. Within a certain range(from once to fifth TCs infections), the higher the number of TCs the larger the volume of tumor growth (Fig 4-F). To verify the interaction mechanism between TCs and HCC cells we designed lentivirus bonded with shRNA to knockdown MMP9 in TCs and knockdown PDGF in HCC cell lines, respectively. The migrations and

invasions of HepG2、SNU182 and SK-HEP-1 cells with shMMP9 TCs were apparently receded compared against these cells with shNC group(Fig 4-I,J) whereas shPDGF cell-lines represented more strong mobility and invasiveness because of compounding with normal MMP9 expression of TCs(Fig 4-G,H). Without MMP9 protein, TCs lost the role of promoting HCC cells' migratory and invasive abilities, of which might be irritated by PDGF protein. To identify our conjecture that TCs played an critical role in distant metastasis of HCC cells, we utilized nude mice to establish lung metastatic lesions from liver cancer and distinguished subgroups according to times of TCs injection from the mouse tail vein(Fig 4-K). We found that the volume of lung metastatic cancer lesions increased with the frequency of TCs injected by HE staining assay(Fig 4-K-a), and meanwhile MMP9 protein expression were more higher in TCs' injection group as contrasted with control group by IHC staining assay(Fig 4-K-b). The body weight of mice in more than twice TCs infection groups decreased after 28 days compared with control group and once group(Fig 4-L). Anatomical observation and the weight of lung rose evidently along with TCs injections compared with control group(Fig 4-M; Fig 4-K-c).

The potential mechanism of PDGF to Telocytes

To explore how PDGF impacted MMP9 expression of TCs, we first tested whether HCC cells secreted MMP9 protein by IHF staining assay, and found that HepG2 cells could only express PDGF protein instead of MMP9 protein(Fig 5-A). In order to explore the concentration gradient of PDGF to facilitate the secretion of MMP9 protein by TCs, we detected the amount of MMP9 secretion by increasing the dose of PDGF and plotted the concentration curve, from which we extracted the most optimal number of TCs cells and PDGF concentration for the following experimental study, so the experiment showed that 5μl of PDGF acting on 6×10^4 TCs resulted in the maximum quantity of MMP9(Fig 5-B). Through previous studies and published literature, we boldly hypothesized that PDGF stimulates TCs to secrete MMP9 by activating the mitrogen-activated protein kinase(MAPK) signaling pathway, so we drew a simulated diagram of extracellular signal-regulated kinase(ERK) signaling pathway to demonstrate the molecular mechanism[37]. In order to verify our conjectures, we utilized PDGF which was the one of agonists for MAPK signaling pathway to stimulate TCs, comparing with resting conditions(NC group) we found that PDGFR as one of TCs membrane receptors transmitted activating information by Son Of Sevenless(SOS) combining with growth-factor-bound-2(Grb2) to motivate downstream effector proteins - Ras/ERK signals. Grb2-sos compound activating, RAF activating and MEK/ERK phosphoylation were shown by Western Blot assay, and finally MMP9 protein was quantitatively expressed(Fig 5-D). Moreover, to demonstrate potent inhibitors of dimeric BRAF, we chose AZ-628[38] which belonged to RAF inhibitors and U0126[39] which belonged to ERK inhibitors to interdict revitalites of MAPK singles, and we found that active RAF, phosphoylative MEK/ERK and MMP9 protein disappeared on the condition of these inhibitors regardless of PDGF(Fig 5-D).

Because miR-942-3p was one of direct targeted gene in regulating MMP9 expression by referring miRbase and TargetScan database, we finally chose miR-942-3p and validated its interaction with MMP9 by Luciferase assay. Differential expression of miR-942-3p in TCs of compared normal liver tissue and hepatocellular carcinoma paracancer tissue was the basis for future study, and we found that miR-942-3p

of TCs separated from HCC para-cancer tissue was more in comparison with normal liver tissue(Fig 5-E). After generating reporter constructs in which 5' UTR mRNA of MMP9 was cloned downstream of the Luciferase open reading frame(Fig 5-F), miR-942-3p could directly combined with MMP9 mRN, in addition mutagenesisi of seed sequences of miR-942-3p binding sites lost the above-mentioned responsiveness(Fig 5-G). Overexpression of miR-942-3p reduced quantities of mRNA and protein of MMP9, whereas miR-942-3p inhibitors reversed these condition(Fig 5-H, J). In line with the result of Western Blot assay, miR-942-3p mimics suppressed TCs to express MMP9 protein, and this competitive effect was overturned by miR-942-3p inhibitors(Fig 5-I).

Additionally, we also detected the cell proliferation and apoptosis of TCs after PDGF stimulated in different phases. There was no significant in TCs' proliferation between with PDGF(1μL) stimulating group and without group(p 0.05) by CCK8 assay in vitro(Suppl. Fig 1-A,B). To determine whether PDGF affects the apoptosis of TCs, we observed apoptosis bodies of TCs during 120hrs after PDGF stimulating by scanning electron microscopy(Suppl. Fig 1-C). Apoptosis bodies occurred on 48hr and visibly appeared on 72hr. Moreover, the expression of cleaved-Caspas3 and Bax were also measured by Western blot assay because these two protein were special characteristics of cell apoptosis, their quantities could signify the level of apoptosis. TCs, stimulated by PDGF, arose apoptosis from 24hr to 96hr as the same time that TCs without PDGF stimulating expressed apoptotic protein(Suppl. Fig 1-D).

Mutation analysis of Telocytes in the HCC para-cancer tissue

Twenty-three specimens from HCC para-cancer tissues and nine normal specimens from perihepatic hemangioma tissues(as somatic gene control analysis) were enrolled in this study. TCs, which were primarily cultured from these samples, were purified to the exon sequence test and analyzed. Low quality reads, junction contamination and reads with high content of unknown base N were removed from the original sequencing data before data analysis(Suppl. Table 3;), and the sample sequencing quality was good as visible by the base quality distribution map(Suppl. Fig 2-A,B). Approximately 60.46 Mb initial bases on target region was captured by the microarray in our experiment, and the mutative test was performed on this target region. The clean reads of each sample were aligned to the reference genome using BWA [Li,2009], and on average 99.9% of the reads were aligned to the reference genome. After removing duplex reads, an average of 54929003 effective reads (8201.91 Mb, effective bases) were obtained(Suppl. Table 4). The average sequencing depth on target was about 86.82X, and 99.71% target regions were covered by at least 1 reads and 96.74% of the target regions were covered by at least 10 reads per sample(Suppl. Table 4; Suppl. Fig 2-C,D). The copy number variants(CNV) in telocytes were also shown with suitable fraction of per reads(Suppl. Fig 2-E).

Each mutation was annotated and predicted function in Human Genome Variation Society (HGVS) nomenclature and pathogenic relationship in COSMIC for somatic mutations. According to exon gene sequences, there were seven types of exon mutations in the somatic TCs compared with TCs in the normal hepatic tissues: 3-prime-UTR mutation(15.25%), 5-prime-UTR mutation(1.69%), splice variants(5.08%), missense mutation(38.98%), frameshift mutation(3.39%), upstream-gene variant(8.47%),

synonymous mutation(27.12%), respectively(Fig 6-A). There were only four sorts of exon mutations of MMPs family in TCs target regain contrast with the control group: SNP-splice mutation(3.33%), SNP-missense(53.33%), SNP-synonymous variant(36.67%), Indel-frameshift mutation(6.67%), respectively(Fig 6-B). The largest proportion type of exome mutation was missense variant. The same sort of MMPs protein possessed distinct SNP exon mutations: MMP1, c.648A>G, T:44A>G; MMP2, c.1149T>C; MMP3, c.1086T>C, c.288T>C; MMP7, c.82C>T, c.230G>A; MMP8, c.95C>T, c.56A>T, c.-80G>C; MMP9, c.1721G>C, c.836A>G, c.1821A>C; MMP11, c.113C>T; MMP12, c.630C>A; MMP14, c.22C>T, c.83T>C; MMP17, c1029G>C, c.423T>C, c.144T>G; MMP19, c.84T>C; MMP21, c.572T>C, c.264G>A; MMP25, c.1622G>A, c.318C>T; MMP27, c.88A>G, c.71C>T, c.797A>T, c.71C>T. Sixteen varieties with thirteen kinds of MMPs protein in TCs(para-cancer tissue originated) were detected as deleterious and pathogenic in COSMIC. Normally, the proportion of SNP missense mutations was the sayingmotto mutative transformation in DNA sequences of TCs(from HCC para-cancer tissue) and played an crucial function on changing final expression of proteins. Moreover, SNP frameshift, synonymous mutation and 3-prime-UTR variant in MMPs family, though not annotated with conflicting significance in database, were classified as non-pathogenic if they couldn't alert the protein domains. Although upstream gene variants, splice accept or region mutation and 5-prime-UTR mutation occurred in MMPs family, they weren't defined lose of function as disease-related gene in COSMIC. Focusing on MMP9 protein mutations, we found that there were two exonic biotypes of missense variants, which betided in Chr20 stating at 44642406 and ending at 44642406, of which codon changes were cGg/cCg as well as cAg/cGg(Suppl. Table 2). So we speculated that cAg/cGg SNP mutation in MMP9 sequence was the reason why TCs from HCC para-cancer tissue could express more MMP9 protein. One synonymous alteration in MMP9 was recorded as "silent biotype" with a low impact of mutative function and wasn't considered as a promoter involved in cancer metastasis progress by impacting MMP9 expression(Suppl. Table 2). Additionally, three specimens of all CNV(copy number variants) tests had mutative changes in exome gene(Suppl. Table 5; Suppl. Fig 2-F).

Discussion

Globally, HCC ranks fourth in cancer-related mortality and is about to overtake breast, prostate and colorectal cancers as the third most common cancer worldwide [2]. In the Asia-Pacific region, the number of new cases of liver cancer in 2020 will be approximately 467,327 [1]. In China, the incidence of HCC remains high for a long time, with 50% of new cases occurring in China, and most patients are already in the progressive stage at the time of consultation. Notwithstanding, China has made great achievements in modern medical development, the incidence and mortality rates of hepatocellular cancer remain high, due to the disadvantageous clinical stage, low surgical resection rates, and high recurrence rates[2]. Metastasis of HCC, incorporating intrahepatic and extrahepatic metastasis, is another main culprit of lethal for patients, by the way to interdict malignant invasiveness into distant organs extensively improves the overall survival[3,4]. We play attention to demonstrate interactions of HCC behavior and surrounding cells, and Telocyte is a fantastic cell type in the progress of cancer metastasis.

In our study, TCs were verified by immunobiology markers CD34, CD117 and PDGFR as well as their morphology on the primary culture as the first step[10]. On account of multiple sub-classifications of MMPs, the expression of MMP-2, 3, 9, 11, 14 were tested by Westen blot and qRT-PCR techniques in the HCC tissue and para-cancer tissue, and then we found that MMP-9 expression was higher in the HCC para-cancer tissue. According to multivariate analysis, high density of TCs and MMP9 expression were correlated with poor overall survival. This result was consistent with previous reports that abnormal MMP-9 expression was associated with tumor malignancy[29] and lymphatic metastasis and clinical stages[40] in breast cancer, as well as close relation with the poor prognosis of primary HCC[41]. Combining with our study, high quantities of TCs and MMP-9 were undoubtedly correlated with HCC invasion and migration. To the contrary, the prognostic model of " high telocytes, low OS" is never absolutely appropriate for all types of malignant tumors: in the breast cancer with BRCA1/2 mutations, the phenomenon of TCs decrease were associated with poor prognosis[42].

Telocytes, belonging to a characteristic and novel type of ICLC, possess ability to interact with HCC cells by secreting signal molecule and various proteins. Telopodes originated from TC's body have ability to transmit cellular information to targeted cells by which was emitted from surrounding cells and circulatory system. These functions of telocytes are calculable basics to participate on changing microenvironment metabolism[43]. Therefore we nervily raise a presumption that TCs might product certain type of MMPs proteins to influence behaviors of tumorigenesis. We found that MMP-9 expression was positive correlation with TCs by Spearman statistic analysis in the HCC para-cancer tissue. TCs were also confirmed to secret MMP-9 in vito. MMP-9 protein have capacity to decompose gelatin and type □, □ and □ collagens which were the barrier of ECM[44], and takes part in the progress of cancer metastasis[45]. The function of TCs was identified in terms of migration and invasion of HCC cells(HepG2, SNU182 and SK-HEP-1 cell lines) by Transwell assay and Wound healing assay, and TCs lost the function with MMP9 inhibitor in vitro and in vivo. Until now, we found the authentic reason to explain that TCs could promote metastasis of HCC through producing and secreting MMP-9.

HCC cells can secret multiple chemokines, growth factors and inflammatory cytokines to impact surrounding cells and change tumor microenvironment(TME), such as vascular endothelial growth factor and PDGF. PDGF is associated with lymphangiogenesis and angiogenesis in gliomas, sarcomas, leukemias and epithelial cancer[46,47]. Chen B proved evidences that PDGF and VEGF expression were implicated with poor prognosis, because HCC cells could secreted them for facilitating cell proliferation, migration and invasion[48]. Based on these facts, we found that PDGF combined with PDGFR which was existed on the surface of TC's cytomembrane and then stimulated TCs to express MMP-9. To illustrate the mechanism of MMP-9 related signal pathway, we refered Kyoto Encyclopedia of Genes and Genomes(KEGG) database to search feasible MMP-9 signal pathways, and determined that PDGF affected MMP-9 expression by ERK signal pathway. By Westen blot assay, PDGF could activate GrB2-sos and Raf in TCs, and contributed to MEK1/2 and ERK1/2 phosphorylation, and finally resulted in MMP-9 expression. This process was obstructed by Raf/ERK diverse inhibitors of AZ-628 and U0126 as a mechanism of down-regulating MMP-9 protein synthesis. As a consequence, we drew a conclusion that TCs promoted the metastasis of HCC through activating ERK signal pathway to express MMP-9 by PDGF

stimulating. Therefore, TCs and HCC cells had a consanguineous association, and TCs were considered as a counterpart of HCC in terms of facilitating invasion and migration of cancer cells. Coincidentally, TC hyperplasia comprising the submucosal thickening characteristic of PDGFRA mutant syndrome, was pathogenetically associated to inflammatory fibroid polyp, and physiological counterpart in the muscularis propria of gastrointestinal stromal tumour[19]. This conclusion and our study jointly elucidate that TCs play an crucial role in the course of oncogenicity and neoplastic circumjacent environment. Inversely, the decrease of TCs also contributed to a genuine fibrosis in Crohn's disease, Ulcerative colitis and liver fibrosis[49].

As is well-known that the ERK signaling pathway belonging to a branch of MAPK pathway is a major and fundamental regulator of human being cells proliferation, apoptosis(cell death) and survival[50]. Growth factor receptor activation induces a series of cascade reactions including phosphorylation and excitation. TCs endlessly accept irritations of diverse growth factor deriving from HCC cells, sustaining sophisticatedly active level of ERK up-regulation, and result in sequential MMP-9 expression which is a vital impetus of invasion an migration of cancer cells. In consideration of multiple functions of ERK signaling for TCs, we detected cell proliferation by CCK-8 staining assay, cell apoptosis by observing apoptotic body under scanning electron microscopy and apoptotic related proteins(Bax and Cleave-caspase-3) by Westen blot method at different phases after PDGF disposing. We investigated that PDGF had no effective influence on TCs' proliferation and apoptosis because amount of TCs with PDGF group in culture were similar to which without PDGF group, and emblematic apoptosis body of TCs still started to appear at 48hrs. Furthermore, the expression of Bax and Cleave-caspase-3 which belong to apoptosis-associated proteins profoundly confirmed aforementioned results. PDGF activation of Raf/ERK signaling pathway is efficient to accelerate MMP-9 expression of TC and promote HCC cell invasion and migration, whereas rarely effective to TC proliferation and apoptosis.

miRNAs pertain to classificatory gene of noncoding RNAs of 18 to 25 nucleotides that decompose mRNA or inhibit translation by the way to bind to the 3'UTR of their target RNAs[51]. Numerous of miRNAs are verified to regulate or control cell biology processes including tumor metastasis, cell division, proliferation and death, directly or indirectly. For instance, miR-128-3p as a tumour suppressor triggers cell cycle arrest by repressing LIMK1 in breast cancer[52], and downregulation of miR-34a reduces HCC metastasis[35]. miRNAs combining to MMP-9 mRNA of TC involve in miR-942-3p, miR-6792, miR-34, and miR-6734 by TargetScan database predicting. In our study, we detected that miR-942-3p in TCs cultured from HCC para-cancer tissue was obviously lower compared with it from normal liver tissue, so we notarized a conclusion that miR-942-3p repressed MMP-9 expression by Luciferase and Westen blot assays as a result of decrease of cell invasion, migration and cancer metastasis. miR-942-3p mimics significantly reduced the expression of MMP-9. Downregulation of mi-942-3p was the mechanism of MMP-9 foison and also the springhead for TCs to promote HCC metastasis.

Up to now, we found tow sorts of molecular mechanisms to decipher interactions between HCC cells and TCs, account for divers MMP-9 expressions and the way for TCs to accelerate cancer metastasis. For TCs, activation of Raf/ERK signaling pathway and downregulation of mi942-3p, respectively, played a

pivotal role in aggrandizing MMP-9 expression and promoting HCC metastasis. Although miR-942 has been reported to regulate various informational pathways and protein expressions, whether miR-942-3p has the function to impress activation or inhibition of ERK signaling pathway and whether PDGF has ability to suppress miR-942-3p synchronously require more investigations in the further.

The discrepancy between annotated protein-coding genes and human polypetides shows an authentic hypothesis of “one-gene, one-polypeptide”. Alternative splicing of gene plays a vital role in protein diversity and protein isoforms complexity[53]. For human beings, up to 95% of multiple exon genes exist mutation to encode proteins during cellular-functions implement[54]. Furthermore, numerous of human hereditary disease and cancers are reported to be correlated with various mutations have capability to change characteristics. MMPs are one of proteins which contribute to the breakdown of extracellular matrix, determining cell migration, proliferation, and metastasis, and MMP-9 is one member of MMPs that is controlled by ERK activity[31]. Diverse mutation analysis about MMPs are reported intermittently through the way of second generation sequencing, but mutative exon gene testing of MMP-9 is still unattended except MMP-9 gene knockdown experiments. The analyse of exon gene sequence fundamentally enhances our understanding of TCs in HCC, provides precise coding gene mutants of TCs and reveals mutation types of MMPs especially MMP-9 gene sequence. Given diverse expression of MMP-9 in TCs(deriving from HCC para-cancer tissue in vitro), we speculated that certain gain-of-function mutations of MMP-9 were intensively correlated with roles of TCs in HCC. We considered that missense mutation and synonymous mutation of MMP-9 exon genes in chromosome 20 resulted in heightening the expression of MMP-9 protein. As a matter of fact, this theory must be confirmed by proteomic analysis and gene splicing technique on the basis of the genre of DNA base and the number of amino acid deletions. These pivotal experiments will demand prompt solutions in the following study.

Paying more attention to the polymorphisms of MMP-9, SNPs constituting substitutions of single bases had been identified in our work as follows: G/C alternation at 1721 position; A/G alternation at 836 position; A/C shift at 1821 position. With respect to previous studies of MMP-9 SNP mutation in -1562 position, C/T SNP shift participated in increasing MMP-9 expression and associating with the invasive phenotype of gastric cancer[55,56] and colon cancer[57]. The MMP-9 -1562CC heterozygous genotype was demonstrated a mark of increased genotype susceptibility to non-small cell lung cancer[58]. Another standpoint on multiple genotypes of MMP-9 SNP was that C/C, C/T and T/T splicing shifts in the pathogenesis and nosetiology of gastric cancer were no significant differences[59]. Furthermore, from dissident theory ecumenical genetic variants in MMP-9 were irrelevant with altered susceptibility of breast cancer in a shanghai breast cancer genetic study[60]. Notwithstanding diverse conceptions in regard to the function of MMP-9 genetic mutations, we persistently deemed that SNPs of MMP-9 in TCs played an crucial role in transforming proteinic expression and promoting metastasis of HCC. In our study, we didn’t monitor -1562 position shift mutation of MMP-9, but -836A/G, -1721G/C and -1821A/C exon gene variants will be considered novel targets to demystify the mechanism of TCs to accelerate invasion and migration of HCC cells, depending on the MMP-9 expression. These preceding targets should be analyzed by the statistic method with age, sex, clinical stage, distant metastasis, OS and histological type parameters in a large cohort of HCC patients in order to support our theory.

Conclusion

Our study started from finding differences of TCs and MMP-9 expression in the HCC tissues, elucidated two potential mechanisms of TCs in promoting the metastasis of HCC cells and stimulating MMP-9 expression in vitro and in vivo:) PDGF from HCC cells activates ERK signaling pathway of TC to enhance MMP-9 expression;) miR-942-3p as a inhibitor suppresses MMP-9 expression. Furthermore, whole exon gene mutations of TCs are tested and analyzed, and MMP-9 related SNPs mutations are detailed detected to explore new targets of TCs.

Abbreviations

HCC: Hepatocellular carcinoma

TCs: Telocytes

ERK: Extracellular signal-regulared protein kinase

MMP9: matrix metalloproteinase-9

ICLC: Interstitial Cajal-like stem cells

PDGFR: Platelet-derived growth factor receptor

ECM: Extracellular matrix

MMPs: matrix metalloproteinases

TGF-β: Transforming growth factor-beta

OS: overall survival

PBS: Phosphate-buffered saline

IHC: Immunohistochemistry

IF: Immunofluorescence

CCK-8: Cell counting kit-8

HE: Hematoxylin and eosin

IGV: Integrative Genomics Viewer

SD: mean ± standard

CNV: Copy number variants

HGVS: Human Genome Variation Society

SNP: Single nucleotide polymorphism

Declarations

Ethics approval: The study was assessed and approved by the Institutional ethic committee of The First Affiliated Hospital of Shandong First Medical University.

Consent for publication: All authors agree to publish this article.

Availability of data and material: All data and material in our research are valid and veritable.

Competing interests: The authors declare no potential conflicts of interest.

Funding: Natural Science Foundation of Shandong Province(ZR2019M

H116)

Author's contributions: Ying Xu carried out the whole studies, participated in all processes of experiments and drafted the manuscript. Hu Tian took charge the authenticity of researches and supported funding. Hua yu Zhang carried out the immunoassays and statistic analysis. Nan Zhang participated in the sequence alignment. Chao guang Luan participated in the design of the study and performed the statistical analysis. Kai Sun conceived of the study, and participated in its design. Peng jin Bao helped to draft the manuscript and drew three pictures and two tables. All authors read and approved the final manuscript.

Acknowledgement We thank all scientists in the Medical Research Center of Shandong Provincial Qianfoshan Hospital.

References

1. Llovet JM, Kelley RK, Villanueva A, Singal AG, Pikarsky E, Roayaie S, Lencioni R, Koike K, Zucman-Rossi J, Finn RS. Hepatocellular carcinoma. Nat Rev Dis Primers. **2021** ;7:6.
2. Lordick F. Hepatocellular carcinoma-united forces against a global killer. Ann Oncol. **2020**;31:449-450.
3. Ko KL, Mak LY, Cheung KS, Yuen MF. Hepatocellular carcinoma: recent advances and emerging medical therapies. F1000Res. **2020** ;9.
4. Piñero F, Dirchwolf M, Pessôa MG. Biomarkers in Hepatocellular Carcinoma: Diagnosis, Prognosis and Treatment Response Assessment. Cells. **2020** ;9:1370.
5. Veress B, Ohlsson B. Spatial relationship between telocytes, interstitial cells of Cajal and the enteric nervous system in the human ileum and colon. J Cell Mol Med. **2020** ;24:3399-3406.

6. Popescu LM, Manole CG, Gherghiceanu M, Ardelean A, Nicolescu MI, Hinescu ME, Kostin S. Telocytes in human epicardium. J Cell Mol Med. **2010**;14:2085-2093.
7. Suciu L, Popescu LM, Gherghiceanu M, Regalia T, Nicolescu MI, Hinescu ME, Faussone-Pellegrini MS. Telocytes in human term placenta: morphology and phenotype. Cells Tissues Organs. **2010**;192:325-339.
8. Hinescu ME, Gherghiceanu M, Suciu L, Popescu LM. Telocytes in pleura: two- and three-dimensional imaging by transmission electron microscopy. Cell Tissue Res. **2011** ;343:389-397.
9. Chen X, Zheng Y, Manole CG, Wang X, Wang Q. Telocytes in human oesophagus. J Cell Mol Med. **2013** ;17:1506-1512.
10. Xu Y, Tian H, Qiao G, Zheng W. Telocytes in the atherosclerotic carotid artery: Immunofluorescence and TEM evidence. Acta Histochem. **2021**;123:151681.
11. Vannucchi MG. The Telocytes: Ten Years after Their Introduction in the Scientific Literature. An Update on Their Morphology, Distribution, and Potential Roles in the Gut. Int J Mol Sci. **2020**;21:4478.
12. Wang L, Xiao L, Zhang R, Jin H, Shi H. Ultrastructural and immunohistochemical characteristics of telocytes in human scalp tissue. Sci Rep. **2020**;10:1693.
13. Rosa I, Marini M, Sgambati E, Ibba-Manneschi L, Manetti M. Telocytes and lymphatic endothelial cells: Two immunophenotypically distinct and spatially close cell entities. Acta Histochem. **2020**;122:151530.
14. Ji S, Traini C, Mischopoulou M, Gibbons SJ, Ligresti G, Faussone-Pellegrini MS. Muscularis macrophages establish cell-to-cell contacts with telocytes/PDGFRα-positive cells and smooth muscle cells in the human and mouse gastrointestinal tract. Neurogastroenterol Motil. **2021**;33:e13993.
15. Usai-Satta P, Bellini M, Morelli O, Geri F, Lai M, Bassotti G. Gastroparesis: New insights into an old disease. World J Gastroenterol. **2020**;26:2333-2348.
16. McCarthy N, Manieri E, Storm EE, Saadatpour A, Luoma AM, Kapoor VN, Madha S, Gaynor LT, Cox C, Keerthivasan S, Wucherpfennig K, Yuan GC, de Sauvage FJ, Turley SJ, Shivdasani RA. Distinct Mesenchymal Cell Populations Generate the Essential Intestinal BMP Signaling Gradient. Cell Stem Cell. **2020**;26:391-402.e395.
17. Gandahi NS, Ding B, Shi Y, Bai X, Gandahi JA, Vistro WA, Chen Q, Yang P. Identification of Telocytes in the Pancreas of Turtles-A role in Cellular Communication. Int J Mol Sci. **2020**;21:2057.
18. Aleksandrovych V, Gil A, Wrona A. Sex steroid hormone receptors of telocytes - potential key role in leiomyoma development. Folia Med Cracov. **2020**;60:81-95.
19. Ricci R, Giustiniani MC, Gessi M, Lanza P, Castri F, Biondi A, Persiani R, Vecchio FM, Risio M. Telocytes are the physiological counterpart of inflammatory fibroid polyps and PDGFRA-mutant GISTs. J Cell Mol Med. **2018**;22:4856-4862.
20. Song D, Xu M, Qi R, Ma R, Zhou Y, Wu D, Fang H, Wang X. Influence of gene modification in biological behaviors and responses of mouse lung telocytes to inflammation. J Transl Med. **2019**;17:158.

21. Rosini S, Pugh N, Bonna AM, Hulmes DJS, Farndale RW, Adams JC. Thrombospondin-1 promotes matrix homeostasis by interacting with collagen and lysyl oxidase precursors and collagen cross-linking sites. Sci Signal. **2018**;11:eaar2566.
22. Yue B. Biology of the extracellular matrix: an overview. J Glaucoma. **2014**;23:S20-23.
23. Cohen L, Sagi I, Bigelman E, Solomonov I, Aloshin A, Ben-Shoshan J. Correction: Cardiac remodeling secondary to chronic volume overload is attenuated by a novel MMP9/2 blocking antibody. PLoS One. **2020**;15:e0241419.
24. Sapa-Wojciechowska A, Rak-Pasikowska A, Pormańczuk K, Czapla B, Bil-Lula I. Extracellular Matrix Remodeling Factors as Markers of Carotid Artery Atherosclerosis. Cardiol Res Pract. **2020**;2020:9036157.
25. Joseph C, Alsaleem M, Orah N, Narasimha PL, Miligy IM, Kurozumi S, et al. Elevated MMP9 expression in breast cancer is a predictor of shorter patient survival. Breast Cancer Res Treat. **2020**;182:267-282.
26. Liang Y, Lv Z, Huang G, Qin J, Li H, Nong F, et al. Prognostic significance of abnormal matrix collagen remodeling in colorectal cancer based on histologic and bioinformatics analysis. Oncol Rep. **2020**;44:1671-1685.
27. Scheau C, Badarau IA, Costache R, Caruntu C, Mihai GL, Didilescu AC, et al. The Role of Matrix Metalloproteinases in the Epithelial-Mesenchymal Transition of Hepatocellular Carcinoma. Anal Cell Pathol (Amst). **2019**;2019:9423907.
28. Wen Y, Cai X, Chen S, Fu W, Chai D, Zhang H, Zhang Y. 7-Methoxy-1-Tetralone Induces Apoptosis, Suppresses Cell Proliferation and Migration in Hepatocellular Carcinoma via Regulating c-Met, p-AKT, NF-κB, MMP2, and MMP9 Expression. Front Oncol. **2020**;10:58.
29. Dong H, Diao H, Zhao Y, Xu H, Pei S, Gao J, et al. Overexpression of matrix metalloproteinase-9 in breast cancer cell lines remarkably increases the cell malignancy largely via activation of transforming growth factor beta/SMAD signalling. Cell Prolif. **2019**;52:e12633.
30. Xuan L, Han F, Gong L, Lv Y, Wan Z, Liu H, et al. Ceramide induces MMP-9 expression through JAK2/STAT3 pathway in airway epithelium. Lipids Health Dis. **2020**;19:196.
31. Marchese V, Juarez J, Patel P, Hutter-Lobo D. Density-dependent ERK MAPK expression regulates MMP-9 and influences growth. Mol Cell Biochem. **2019**;456:115-122.
32. Kaomongkolgit R, Cheepsunthorn P, Pavasant P, Sanchavanakit N. Iron increases MMP-9 expression through activation of AP-1 via ERK/Akt pathway in human head and neck squamous carcinoma cells. Oral Oncol. **2008**;44:587-594.
33. Sanches BDA, Maldarine JDS, Tamarindo GH, Da Silva ADT, Lima MLD, Rahal P, et al. Explant culture: A relevant tool for the study of telocytes. Cell Biol Int. **2020**;44:2395-2408.
34. Romano E, Rosa I, Fioretto BS, Lucattelli E, Innocenti M, et al. A Two-Step Immunomagnetic Microbead-Based Method for the Isolation of Human Primary Skin Telocytes/CD34+ Stromal Cells. Int J Mol Sci. **2020**;21:5877.

35. Li N, Fu H, Tie Y, Hu Z, Kong W, Wu Y, et al. miR-34a inhibits migration and invasion by down-regulation of c-Met expression in human hepatocellular carcinoma cells. Cancer Lett. **2009**;275:44-53.
36. Xu Y, Tian H, Cheng J, Liang S, Li T, et al. Immunohistochemical biomarkers and distribution of telocytes in ApoE-/- mice. Cell Biol Int. **2019**;43:1286-1295.
37. Marchese V, Juarez J, Patel P, Hutter-Lobo D. Density-dependent ERK MAPK expression regulates MMP-9 and influences growth. Mol Cell Biochem. **2019**;456:115-122.
38. McDermott U, Sharma SV, Dowell L, Greninger P, Montagut C, Lamb J, et al. Identification of genotype-correlated sensitivity to selective kinase inhibitors by using high-throughput tumor cell line profiling. Proc Natl Acad Sci U S A. **2007**;104:19936-19941.
39. Duan W, Chan JH, Wong CH, Leung BP, Wong WS. Anti-inflammatory effects of mitogen-activated protein kinase kinase inhibitor U0126 in an asthma mouse model. J Immunol. **2004**;172:7053-7059.
40. Li H, Qiu Z, Li F, Wang C. The relationship between MMP-2 and MMP-9 expression levels with breast cancer incidence and prognosis. Oncol Lett. **2017**;14:5865-5870.
41. Cao S, Zhu S, Yin W, Xu H, Wu J, et al. Relevance of EGFR Between Serum VEGF and MMP-9 in Primary Hepatocellular Carcinoma Patients with Transarterial Chemoembolization. Onco Targets Ther. **2020**;13:9407-9417.
42. Mihalcea CE, Moroşanu AM, Murăraşu D, Puiu L, Cinca SA, er al. Molecular analysis of BRCA1 and BRCA2 genes by next generation sequencing and ultrastructural aspects of breast tumor tissue. Rom J Morphol Embryol. **2017**;58:445-455.
43. Cretoiu D, Cretoiu SM, Simionescu AA, Popescu LM. Telocytes, a distinct type of cell among the stromal cells present in the lamina propria of jejunum. Histol Histopathol. **2012**;27:1067-1078.
44. Bronisz E, Kurkowska-Jastrzębska I. Matrix Metalloproteinase 9 in Epilepsy: The Role of Neuroinflammation in Seizure Development. Mediators Inflamm. **2016**;2016:7369020.
45. Mondal S, Adhikari N, Banerjee S, Amin SA, Jha T. Matrix metalloproteinase-9 (MMP-9) and its inhibitors in cancer: A minireview. Eur J Med Chem 2020;194:112260.
46. Senga SS, Grose RP. Hallmarks of cancer-the new testament. Open Biol. **2021**;11:200358.
47. Yuge R, Kitadai Y, Shinagawa K, Onoyama M, Tanaka S, et al. mTOR and PDGF pathway blockade inhibits liver metastasis of colorectal cancer by modulating the tumor microenvironment. Am J Pathol. **2015**;185:399-408.
48. Chen B, Liu J, Wang X, Shen Q, Li C, et al. Co-expression of PDGF-B and VEGFR-3 strongly correlates with poor prognosis in hepatocellular carcinoma patients after hepatectomy. Clin Res Hepatol Gastroenterol. **2018**;42:126-133.
49. Ibba-Manneschi L, Rosa I, Manetti M. Telocytes in Chronic Inflammatory and Fibrotic Diseases. Adv Exp Med Biol. **2016**;913:51-76.
50. Wu PK, Becker A, Park JI. Growth Inhibitory Signaling of the Raf/MEK/ERK Pathway. Int J Mol Sci. **2020**;21:5436.

51. Goodall GJ, Wickramasinghe VO. RNA in cancer. Nat Rev Cancer. **2021**;21:22-36.
52. Zhao J, Li D, Fang L. MiR-128-3p suppresses breast cancer cellular progression via targeting LIMK1. Biomed Pharmacother. **2019**;115:108947.
53. Graveley BR. Alternative splicing: increasing diversity in the proteomic world. Trends Genet. **2001**;17:100-107.
54. Pan Q, Shai O, Lee LJ, Frey BJ, Blencowe BJ. Deep surveying of alternative splicing complexity in the human transcriptome by high-throughput sequencing. Nat Genet. **2008**;40:1413-1415.
55. Verma S, Kesh K, Gupta A, Swarnakar S. An Overview of Matrix Metalloproteinase 9 Polymorphism and Gastric Cancer Risk. Asian Pac J Cancer Prev. **2015**;16:7393-7400.
56. Matsumura S, Oue N, Nakayama H, Kitadai Y, Yoshida K, Yamaguchi Y, et al. A single nucleotide polymorphism in the MMP-9 promoter affects tumor progression and invasive phenotype of gastric cancer. J Cancer Res Clin Oncol. **2005**;131:19-25.
57. Banday MZ, Sameer AS, Mir AH, Mokhdomi TA, Chowdri NA, et al. Matrix metalloproteinase (MMP) -2, -7 and -9 promoter polymorphisms in colorectal cancer in ethnic Kashmiri population - A case-control study and a mini review. Gene. **2016**;589:81-89.
58. Li W, Jia MX, Wang JH, Lu JL, Deng J, et al. Association of MMP9-1562C/T and MMP13-77A/G Polymorphisms with Non-Small Cell Lung Cancer in Southern Chinese Population. Biomolecules. **2019**;9:107.
59. Avcı N, Ture M, Deligonul A, Cubukcu E, Olmez OF, et al. Association and Prognostic Significance of the Functional -1562C/T Polymorphism in the Promoter Region of MMP-9 in Turkish Patients with Gastric Cancer. Pathol Oncol Res. **2015**;21:1243-1247.
60. Beeghly-Fadiel A, Lu W, Shu XO, Long J, Cai Q, Xiang Y, et al. MMP9 polymorphisms and breast cancer risk: a report from the Shanghai Breast Cancer Genetics Study. Breast Cancer Res Treat. **2011**;126:507-13.

Tables

Table 1 Comparison between low and high telocyte groups of HCC patients. The statistic had significant when p<0.05□MMP9□Matrix metalloproteinase-9

	Low-Telocyte(n=38)	High-Telocyte(n=94)	*t/p* value
Age,Mean±SD,years	75.763±1.640	65.510±0.934	45.25/0.001
Sex,Male/Female	16/22	55/39	
Metastasis, number(%)			
M_1	12(31.6)	82(87.2)	
M_0	26(68.4)	12(12.7)	
MMP9,Mean±SD,um2/mg/mm3	7.138±0.273	7.859±0.349	13.66/0.001
OS,Mean±SD,months	17.234±3.290	9.263±2.606	13.33/0.000

Table 2 Multivariate analysis of overall survival in HCC patients. The statistic had significant when p<0.05MMP9Matrix metalloproteinase-9; TCs:Telocytes;HR: hazard ratio; CI: confidence interval; HCC: hepatocellular carcinoma

	HR	95%CI	Mutivariate P-value
Age	0.633	0.453-0.905	0.077
Sex	0.759	0.536-1.032	0.106
Metastasis	0.402	0.270-0.577	0.000
MMP9 (para-cancer tissue)	0.572	0.480-0.993	0.001
TCs (para-cancer tissue)	0.698	0.412-0.891	0.001

Table 3 Pearson's correlation of MMP-9 expression and telocyte number in HCC tissues. The analysis implies significant positive correlation between the two factors. The correlation between MMP-9 protein and telocytes is significant . a is in the cancer tissues(*p < 0.05), and b is in the para-cancer tissues(**p < 0.05).

		Telocyte number
MMP-9 expression	Correlation coefficient	0.898*
		0.687**
	Significance (p value)	0.011[a]
		0.001[b]

Figures

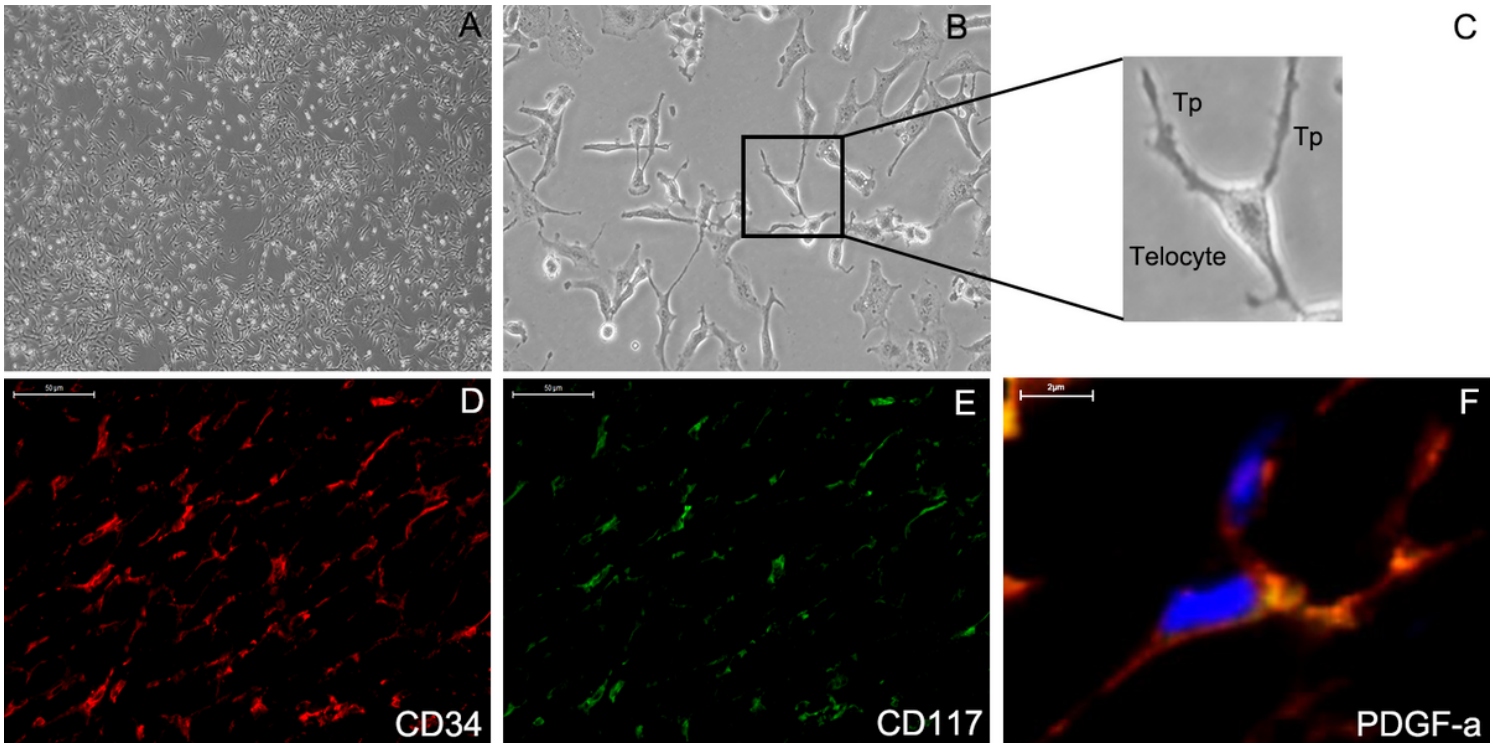

Figure 1

The morphology and immunoflurescent staining of TCs. The unique morphology of TCs were showed under the light microscopy(×40, A; ×200, B). The long and thin extending feature was named telopode(×400) and there were three telopodes from TC's body(C). TCs were positive for CD34(red, D), CD117(green, E) and PDGF-α(yellow, F). Tp:telopode

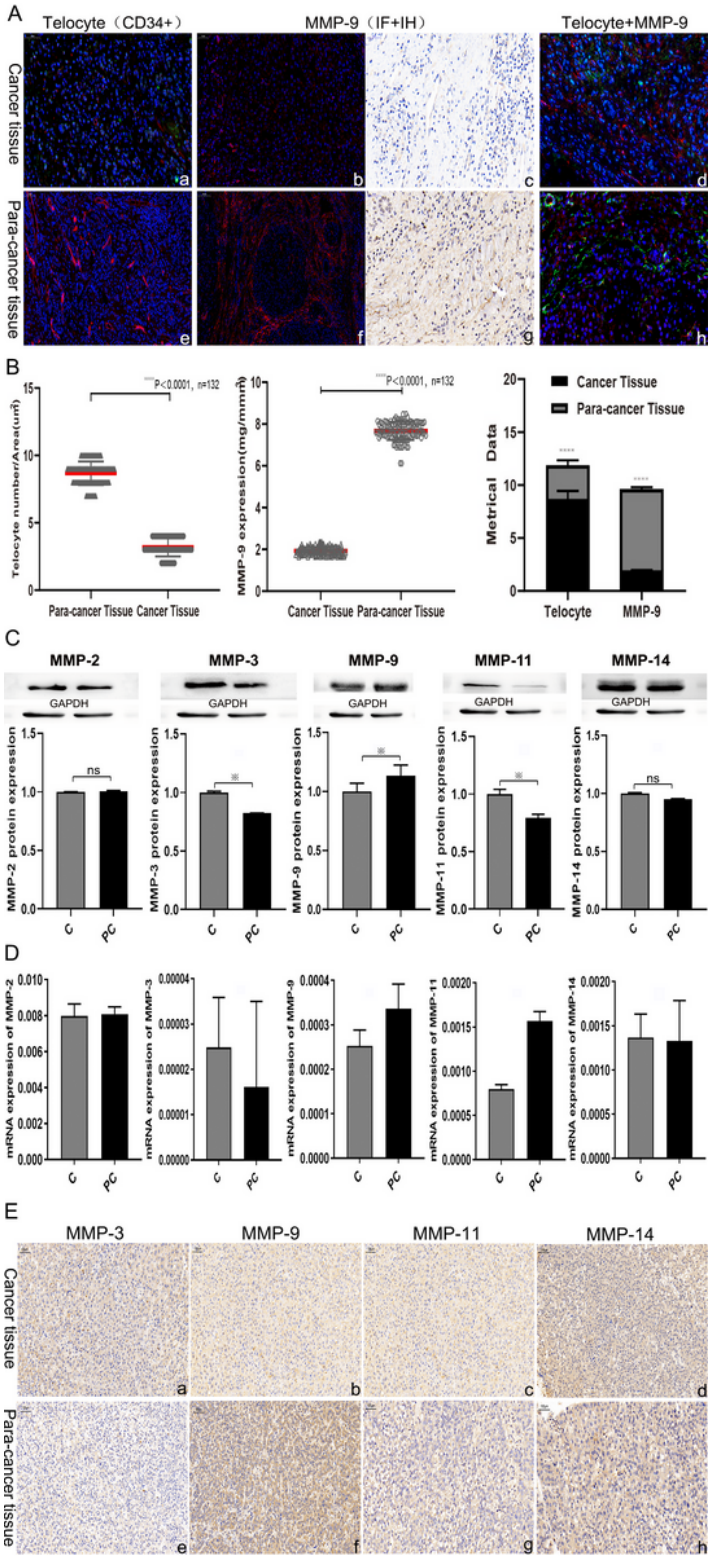

Figure 2

The difference of telocytes and MMP-9 protein expression in the hepatocellular cancer tissue and para-cancer tissue. A: CD34 positive telocytes(red) in the HCC tissue and para-cancer tissue(a,e). MMP-9 protein expression in paired-tissues by immunohistochemistry and immunofluorescence assays(b,c,f,g). The relationship and distribution of telocytes(CD34+,green) and MMP-9 protein(red) in the same paired-tissue by immunofluorescence assay(d,h). B: The accurately quantities of telocytes and MMP-9 protein

expression have statistical significance in the 132 paired specimens of HCC and para-HCC tissues(※※※※p<0.0001). C: Partial MMPs protein family, including MMP2, MMP3, MMP9, MMP11 and MMP14, express in the HCC tissues compared with para-HCC tissues by Westen Blot technique(n=132). GAPDH as the concentration. D: qRT-PCR analysis represents distinct MMPs protein expression in the HCC tissues. E: Different expression of partial MMPs protein family in the cancer and para-cancer tissue according to the immunohistochemistry assay. Star marker represents that datum have statistically significant, p<0.05. The scar bar is 50μm in A, 100μm in E, respectively. Data represents means ± SD, and level of significance is determined using paired t-test.

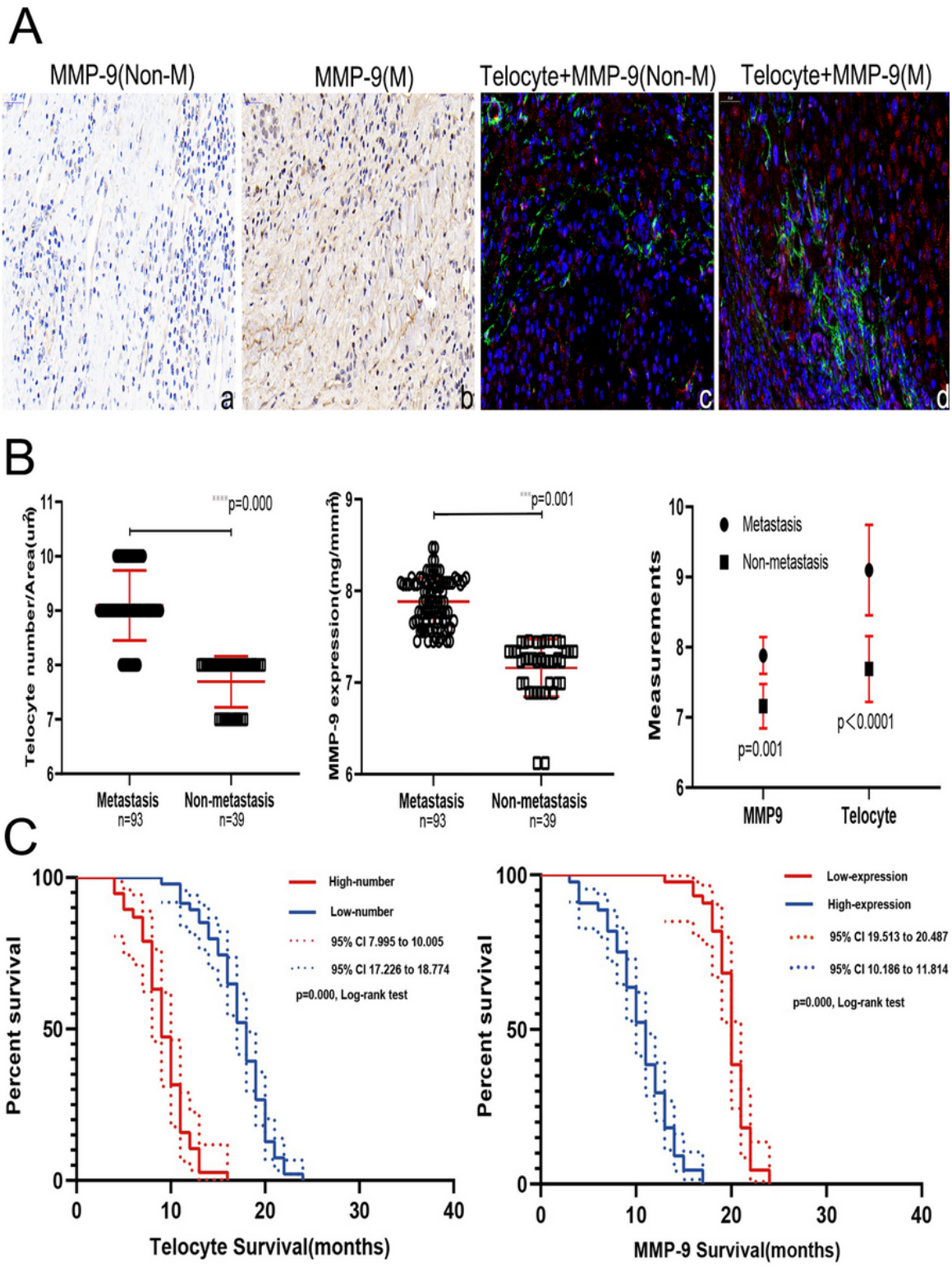

Figure 3

Telocytes and MMP-9 protein expression in the HCC para-cancer tissues between metastasis group and non-metastasis group. A: MMP-9 protein expression represents distinctly in the HCC tissue with non-metastasis(a) and metastasis(b) by immunohistochemistry staining. The relationship and distribution between telocytes(green) and MMP-9 protein(red) in the para-cancer tissue are disparate with non-metastasis(c) and metastasis(d) by immunofluorescence staining . B: The levels of telocytes and MMP-9

protein in the metastasis group(n=93) and non-metastasis group(n=39), and the differences have statistically significant. C: Kaplan-Meier analysis of overall survival in HCC patients(n=265) with a low(red line) or high(blue line) level of telcoyte(left panel) and MMP-9 protein(right panel), respectively(p<0.05, Log-rank test). ※※※※p<0.001, ※※※p=0.001

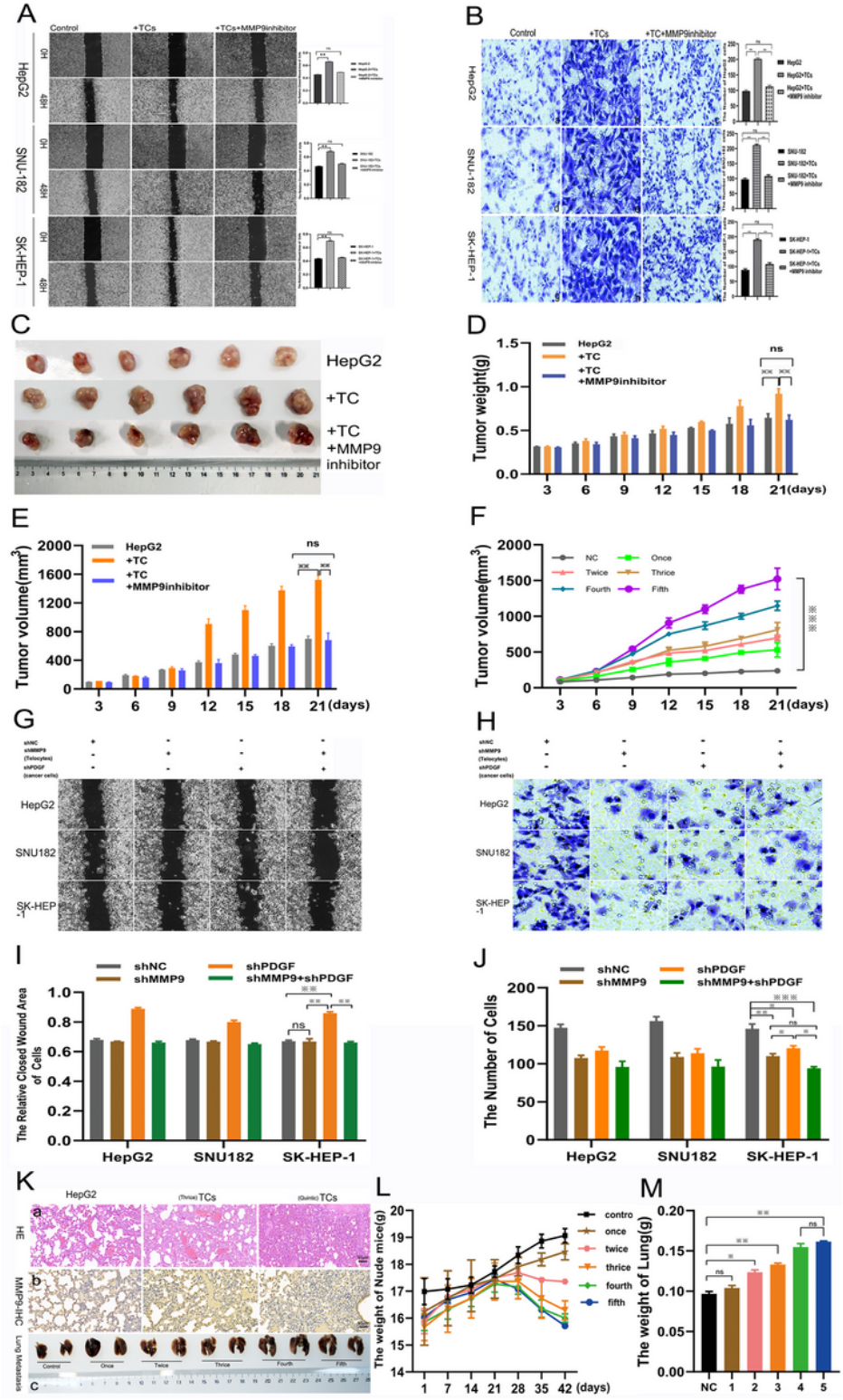

Figure 4

Telocytes promoted metastasis of cancer depending on MMP-9 protein. TCs promoted migrations of hepatic cancer cells by the Wound healing assay(A) and facilitated invasions of hepatic cancer cells by the Transwell assay(B). Representative photos of xenograft tumor in vivo(C), growth curves of tumor weight(D) and volume(E) over time in HepG2 group, adding TCs group, adding TCs and MMP9 inhibitor group. Tumor growth curves of volumes with incremental injections of TCs(F). Knockdown MMP9 in TCs and knockdown PDGF in HCC influenced migrations and invasions of hepatic cancer cells after 48 hours by Wound healing and Transwell assays(G,H). The number of migratory cells(I) and invasive cells(J) were calculated in shMMP9 and shPDGF groups. Representative photographs of metastatic lung tissues derived from HepG2 cancer cells with distinct frequencies of TCs' injection by HE staining(K-a) and in vivo(K-c). The expression of MMP9 by IHC staining were shown in different groups(K-b). Contrast curves of the nude mice weight(L) and the weight of metastatic lung tissues(M) with distinct frequencies of TCs' injections. ns: no significance; ※p<0.05, ※※p<0.01, ※※※p<0.005.

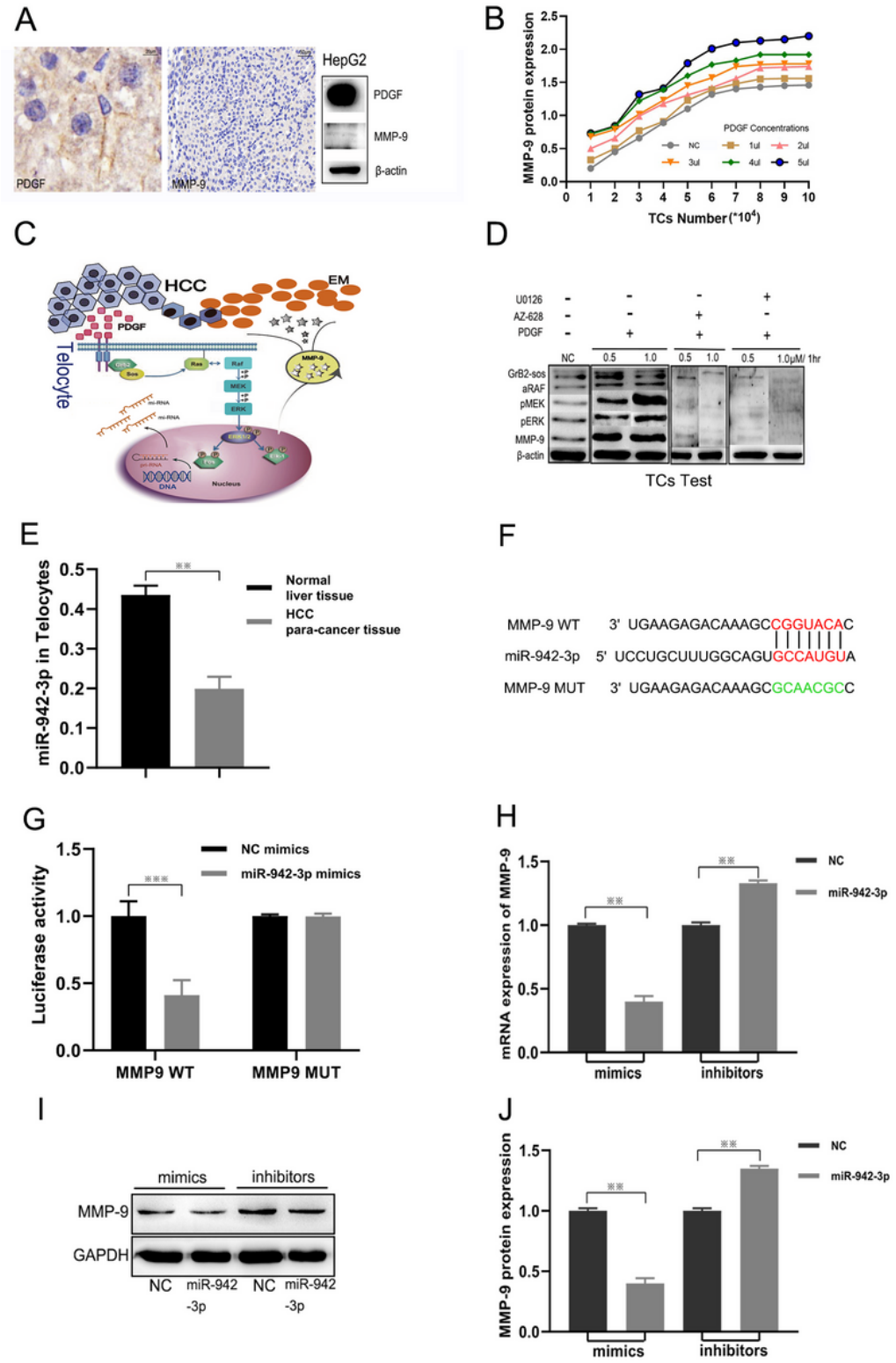

Figure 5

Ras/ERK signal pathway and miR-942-3p regulated MMP9 expression in telocytes. HepG2 cells secreted PDGF but not MMP9(A). MMP9 protein expression were measured in the different quantities of TCs and different concentrations of PDGF(B). Simulation of the mechanism of MMP9 secretion by TC including Ras/ERK signal pathway and relative miRNA(C). PDGF stimulated TCs to express MMP9 protein according to activate Ras/ERK signal pathway that inhibited by U0126 and AZ-628(D). Distinctive

expression of miR-942-3p in TCs between HCC para-cancer tissue and normal liver tissue(E). Predicted binding site between miR-942-3p and the 5' UTR sequence of MMP9, as well as artificial mutative sites of MMP9(F). The relative binding evident among miR-942-3p, 5' UTR of MMP9 mRNA and mutative type of MMP9 mRNA by luciferase reporter gene assay(G). Measurements of MMP9 incorporating mRNA and protein in TCs after miR-942-3p was overexpressed or inhibited(H, J). Differential expression of MMP9 with miR-942-3p mimics or inhibitors by Westen Blot assay(I).

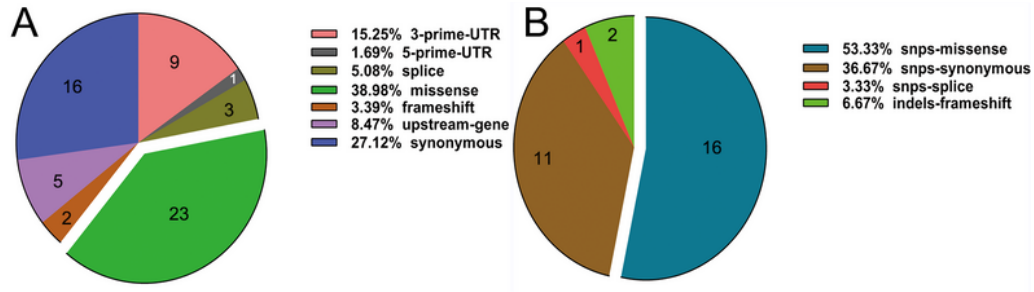

C

Function	Gene	Varient	COSMIC	Chr
frameshift	MMP12	NM_002426.4:p.Thr211_Cys212fs/c.631_632insA	COSM1350419(2)	chr11
	MMP28	NM_024302.4:p.Leu146_Arg147fs/c.437_438insG		chr17
missense	MMP10	NM_002425.2:p.Arg53Lys/c.158G>A		chr11
	MMP11	NM_005940.3:p.Ala38Val/c.113C>T	COSM1751756(10)	chr22
	MMP14	NM_004995.3:p.Pro8Ser/c.22C>T	COSM432856(3)	chr14
	MMP17	NM_016155.4:p.Ala182Thr/c.544G>A; Arg279His/c.836G>A	COSM3753055(4)	chr12
	MMP20	NM_004771.3:p.Thr281Asn/c.842C>A; Val275Ala/c.824T>C; Lys18Thr/c.53A>C; Val275Ala/c.824T>C; Lys18Thr/c.53A>C; Thr281Asn/c.842C>A; Val275Ala/c.824T>C		chr11
	MMP21	NM_147191.1:p.Val191Ala/c.572T>C	COSM3751596(2)	chr10
	MMP25	NM_022468.4:p.Gly541Glu/c.1622G>A	COSM3754861(1)	chr16
	MMP27	NM_022122.2:p.Met30Val/c.88A>G; Thr24Met/c.71C>T; Glu266Val/c.797A>T; Thr24Met/c.71C>T	COSM1579495(1)	chr11
	MMP7	NM_002423.3:p.Arg77His/c.230G>A	COSM3752093(1)	chr11
	MMP8	NM_002424.2:p.Lys87Glu/c.259A>G; Thr32Ile/c.95C>T		chr11
	MMP9	NM_004994.2:p.Arg574Pro/c.1721G>C; Gln279Arg/c.836A>G	COSM3758601(1)	chr20
synonymous	MMP1	NM_002421.3:p.Ala216Ala/c.648A>G		chr11
	MMP10	NM_002425.2:p.Ile362Ile/c.1086C>A; Phe162Phe/c.486T>C	COSM3752099(1)	chr11
	MMP12	NM_002426.4:p.Thr210Thr/c.630C>A		chr11
	MMP17	NM_016155.4:p.Arg343Arg/c.1029G>C		chr12
	MMP19	NM_002429.5:p.Pro28Pro/c.84T>C		chr12
	MMP2	NM_004530.4:p.Asp383Asp/c.1149T>C	COSM4129119(1)	chr16
	MMP21	NM_147191.1:p.Ala88Ala/c.264G>A		chr10
	MMP25	NM_022468.4:p.Arg106Arg/c.318C>T	COSM3754852(5)	chr16
	MMP27	NM_022122.2:p.Gly409Gly/c.1227G>A	COSM428286(1)	chr11
	MMP3	NM_002422.3:p.Ala362Ala/c.1086T>C; Asp96Asp/c.288T>C	COSM3752100(1)	chr11
	MMP9	NM_004994.2:p.Gly607Gly/c.1821A>C	COSM3749712(10)	chr20
upstream_gene	MMP13	NM_002427.3		chr11
	MMP7	NM_002423.3		chr11
	MMP7	NM_002423.3		chr11
	MMP8	NM_002424.2		chr11
splice_acceptor	MMP10	NM_002425.2:c.497A>G		chr11
splice_region	MMP17	NM_016155.4:c.423T>C		chr12
3_prime_UTR	MMP1	NM_002421.3:c.*63C>T; 44A>G	COSN164034	chr11
	MMP10	NM_002425.2:c.*142C>T		chr11
	MMP14	NM_004995.3:c.*83T>C		chr14
	MMP17	NM_016155.4:c.*144T>G		chr12
	MMP7	NM_002423.3:c.*82C>T		chr11
	MMP8	NM_002424.2:c.*56A>T		chr11
5_prime_UTR	MMP8	NM_002424.2:c.-80G>C		chr11

Figure 6

Exome gene mutations of telocytes in the HCC para-cancer tissue. All types of exome gene mutation of TCs(A). Exome mutations' ratio of MMPs protein family in TCs(B). Details of MMPs protein family mutations in TCs(C).

Supplementary Files

This is a list of supplementary files associated with this preprint. Click to download.

- renamed546f3.tif
- renamed73855.tif